

# **Laser properties of Nd:FAP and Nd:S-FAP ceramics at 1.06 and 1.33 $\mu\text{m}$**

Kazuya Takimoto<sup>1,2</sup>, Hiroyasu Sone<sup>2</sup>, and Hiroaki Furuse<sup>1\*</sup>

<sup>1</sup> *National Institute for Materials Science, Tsukuba, Ibaraki 305-0047, Japan*

<sup>2</sup> *Kitami Institute of Technology, Kitami, Hokkai-do 090-8507, Japan*

\*E-mail: FURUSE.Hiroaki@nims.go.jp

The laser properties of Nd-doped  $\text{Ca}_{10}(\text{PO}_4)_6\text{F}_2$  (FAP) and  $\text{Sr}_{10}(\text{PO}_4)_6\text{F}_2$  (S-FAP) ceramics with a hexagonal (non-cubic) crystal structure were investigated at 1.06- and 1.33- $\mu\text{m}$  wavelength ranges. Slope efficiencies of 10.1% and 11.7% were obtained for FAP and S-FAP ceramics at 1063 and 1059 nm, respectively. To the best of our knowledge, slope efficiency of over 10% is the highest among non-cubic ceramic materials. Additionally, laser oscillations at 1335 and 1327 nm were observed in FAP and S-FAP ceramics, respectively. The results of this study will be valuable for future advancements in achieving higher power and efficient operation of non-cubic laser ceramics.

Fluorapatite ( $\text{Ca}_{10}(\text{PO}_4)_6\text{F}_2$ : FAP) single crystals, which possess a hexagonal crystal structure, were actively studied as laser host materials. Laser oscillation was first achieved with a Nd:FAP single crystal in 1968<sup>1)</sup> and with Nd-doped strontium fluorapatite, S-FAP ( $\text{Sr}_{10}(\text{PO}_4)_6\text{F}_2$ ), in 1972.<sup>2)</sup> Subsequently, research has actively focused on achieving a higher power output<sup>3-5)</sup>, detailed characterization<sup>6,7)</sup> and Q-switched oscillation.<sup>8)</sup> Furthermore, Yb:S-FAP single crystals have been developed as high-power laser materials and employed in laser inertial fusion drivers.<sup>9,10)</sup>

In recent years, transparent yttrium-aluminum-garnet (YAG) ceramics have become mainstream laser host materials for high-average-power laser sources. In fact, outputs exceeding 150-J pulse energy—with a 10 Hz repetition rate and an average output power of 1.5 kW—have been achieved.<sup>11)</sup> The advantages of polycrystalline ceramic technology include size scalability, the ability to realize composite materials, optical uniformity, and high mechanical strength. However, since polycrystalline ceramics consist of multiple crystal grains, it is generally considered that laser quality can only be attained with optically isotropic (cubic) materials because they are unaffected by birefringence.<sup>12)</sup>

Non-cubic ceramic materials, such as hexagonal FAP, have the potential to be utilized as high-power laser materials. The extent of grain boundary scattering resulting from birefringence, denoted as  $\gamma$ , is described by the following equation<sup>13)</sup>:

$$\gamma(\lambda) = \frac{3\pi^2 d \Delta n^2}{2\lambda^2}, \quad (1)$$

where  $d$  is the average grain size,  $\Delta n$  is the average difference in refractive index at the grain boundaries, and  $\lambda$  is the wavelength of light. Akiyama et al. first demonstrated laser oscillation in non-cubic ceramics using Nd:FAP in 2011<sup>14,15)</sup> by employing a crystal orientation alignment to reduce  $\Delta n$ . Sato et al. fabricated transparent Yb:FAP ceramics using the same approach<sup>16)</sup> and successfully achieved Q-switched laser operation, attaining a maximum peak power of 2.3 kW in 2017.<sup>17)</sup>

Alternatively, we aimed to achieve transparent rare-earth (RE = Nd, Yb)-doped FAP and S-FAP ceramics by controlling the average grain size  $d$  to approximately 100 nm.<sup>18-20)</sup> Laser oscillations for Nd:FAP, Nd:S-FAP, and Yb:FAP were demonstrated at the 1  $\mu\text{m}$  wavelength range, despite the ceramics being composed of randomly oriented crystal grains. However, the maximum slope efficiency obtained was only 6.5%, suggesting the potential for further enhancement.

Systematically varying the output coupler (OC) to optimize laser performance is an effective strategy because the laser output power and slope efficiency are dependent on the

cavity configuration, including the reflectivity of the OC. Additionally, to the best of our knowledge, Nd-doped materials can emit at 1.33  $\mu\text{m}$ ; however, laser oscillation from apatite has only been reported in Nd:S-FAP single crystals.<sup>4)</sup> Demonstrating laser oscillation at various wavelengths is crucial for expanding the potential of non-cubic ceramics as efficient laser materials. In light of this, our objective was to enhance laser efficiencies at 1.06  $\mu\text{m}$  by optimizing the reflectivity of the OC, and to demonstrate oscillation in the 1.33  $\mu\text{m}$  wavelength range for both Nd:FAP and Nd:S-FAP transparent ceramics.

Transparent Nd:FAP and Nd:S-FAP laser ceramics were fabricated using a process similar to that in our previous studies.<sup>18,20)</sup> The thicknesses of the Nd:FAP and S-FAP used for laser testing in this study were 1.0 and 0.6 mm, respectively. The loss coefficients of the ceramics at 1.06  $\mu\text{m}$ , derived from in-line transmittance, were 0.4  $\text{cm}^{-1}$  for both Nd:FAP and Nd:S-FAP. Thus, these ceramics exhibited approximately identical optical qualities.

Figure 1 shows the experimental setup used for the laser oscillation test. A laser cavity of approximately 1 mm length was configured with a flat dichroic mirror (DM) and an OC, with the ceramic sample attached to the DM. Note that the sample was not treated with an anti-reflection (AR) coating, and no cooling system was implemented in this study. A 60 W continuous wave (CW) fiber-coupled laser diode (LD) served as the pump source. The core diameter of the fiber was 105  $\mu\text{m}$  and the numerical aperture (NA) was 0.22. The wavelength of LD was adjusted via temperature control to match the absorption peaks of Nd:FAP (807 nm) and Nd:S-FAP (805 nm). To prevent thermal issues, the LD was operated in the quasi-continuous wave (QCW) mode with a pulse width of 1 ms and a repetition rate of 10 Hz, corresponding to a duty ratio of 1%.

To measure laser oscillation at 1.06  $\mu\text{m}$ , various OC reflectivities ( $R = 99\%, 95\%, 90\%, 85\%, 80\%$ , and  $70\%$ ) were used to determine the maximum slope efficiency. In the oscillation test at a wavelength of 1.33  $\mu\text{m}$ , the availability of commercial optical components was more limited than that at 1.06  $\mu\text{m}$ . This limitation poses challenges in preparing a diverse range of output mirrors, as was achieved in the 1.06  $\mu\text{m}$  experiments. Consequently, an OC with 90% reflectivity at 1.33  $\mu\text{m}$  was used. The laser output power, laser spectrum, and beam profile were measured using a thermopile power meter (PM: 3A, Ophir), an optical spectrum analyzer (OSA: Q8383, Advantest), and a CMOS camera (SP932U, Ophir).

Figures 2(a) and (b) show the laser output power at 1.06  $\mu\text{m}$  wavelength as a function of absorbed pump power for various OC reflectivities. The insets display the typical lasing

spectra. The laser wavelengths were 1063 and 1059 nm for Nd:FAP and Nd:S-FAP, respectively, which were consistent with those observed in single crystals.<sup>3-7)</sup> The highest slope efficiencies of 10.1% for Nd:FAP and 11.7% for Nd:S-FAP were obtained at 85% OC. To the best of our knowledge, these represent the highest slope efficiencies reported for non-cubic laser ceramics.

In general, the laser power  $P_{out}$  can be evaluated using the following equation<sup>21)</sup>:

$$P_{out} = A \left( \frac{1-R}{1+R} \right) I_s \left( \frac{2g_0 l}{\delta - \ln R} - 1 \right), \quad (2)$$

where  $A$  is the beam cross section,  $R$  is the reflectivity of the OC,  $I_s$  is the saturation fluence,  $g_0$  is the small signal gain coefficient,  $l$  is the sample thickness, and  $\delta$  is the round-trip loss within the cavity.

Figure 3 shows the correlation between laser power and OC reflectivity for Nd:FAP and S-FAP. The results are presented for the maximum pump power (283 mW for Nd:FAP and 153 mW for Nd:S-FAP). The dotted lines in Figure 3 are the fitting curves derived from Eq. (2) with  $2g_0 l$  and  $\delta$  as fitting parameters, where  $A = 8.65 \times 10^{-5} \text{ cm}^2$  corresponding to a 105  $\mu\text{m}$  core area, and  $I_s = 4093 \text{ W/cm}^2$ .<sup>20)</sup> The fitting results showed good agreement with the experimental results, at the values of  $2g_0 l = 1.04 \pm 0.09$  and  $\delta = 0.42 \pm 0.06$  for Nd:FAP, and  $2g_0 l = 0.85 \pm 0.11$  and  $\delta = 0.40 \pm 0.08$  for Nd:S-FAP.

Although the estimated values of cavity losses,  $\delta$ , exceeded 40%, this value includes Fresnel losses of 21.5% at the ceramic surfaces. In the configurations used in this study, where thin laser materials without AR coatings and very short laser cavities are employed, there is a potential for multiple reflections and interference occur at the optical surfaces within the cavity. In future, we will apply AR coatings, introduce a cooling system, and utilize a stable laser cavity in similar experiments to facilitate a more detailed analysis and deepen our understanding of the characteristics of non-cubic ceramic lasers.

Figures 4(a) and (b) show the laser beam profiles and  $M^2$ -fit curves for the Nd:FAP and Nd:S-FAP ceramics, respectively. For this measurement, the laser beam profiles at the same pumping power of 170 mW—with corresponding absorbed pump powers of 94 mW and 47 mW for Nd: FAP and Nd:S-FAP, respectively—were measured using a lens with a focal length of 100 mm. The  $1/e^2$  value of the beam size at each measurement point was used to evaluate  $M^2$ , as shown in Figure 4. The  $M^2$  values for Nd:FAP and Nd:S-FAP were approximately 1.2 when the pump power was relatively low, confirming that a Gaussian-like beam was obtained under these experimental conditions.

Figure 4(c) shows the  $M^2$  values and near-field patterns (NFP) of Nd:S-FAP at absorbed

pump powers of 34 mW, 94 mW, and 153 mW. The spatial interference fringes in the NFP are attributed to the ND filter positioned in front of the CMOS camera. This figure indicates that the beam quality degraded with increasing pumping power. We also attempted to conduct the same experiment for Nd:FAP; however, the experiment led to material damage, which prevented measurements from being obtained. This suggests that the material is affected by thermal effects, as Nd:FAP absorbed higher pump power owing to its thickness, which could be improved by the future implementation of a cooling system for the sample.

Figure 5(a) shows the laser power at 1.33  $\mu\text{m}$  wavelength range as a function of absorbed pump power. To the best of our knowledge, this is the first laser oscillation from Nd:FAP in the 1.33  $\mu\text{m}$  wavelength range. A maximum output power of 9 mW, which corresponds to a peak power of 0.9 W, was obtained. Slope efficiencies of Nd:FAP and S-FAP were 4.8% and 5.4%, respectively. Figure 5(b) shows laser and emission spectra for Nd:FAP and Nd:S-FAP ceramics, respectively. The laser wavelengths for Nd:FAP and Nd:S-FAP ceramics were 1335 and 1327 nm, respectively. These lasing spectra were in good agreement with the fluorescence peak of Nd:FAP single crystal (1334.8 nm)<sup>1)</sup> and the laser spectrum of Nd:S-FAP single crystal (1327 nm).<sup>4)</sup>

Table 1 summarizes the laser characteristics, including the laser wavelength, slope efficiency, and output average power for the Nd:FAP and S-FAP ceramics. For comparison, the values of the corresponding single crystals are also listed.<sup>3,4)</sup> In the 1.06  $\mu\text{m}$  wavelength range, the maximum slope efficiencies of the ceramics were approximately 10% (10.1% for FAP and 11.7% for S-FAP), which were approximately one-fifth of the values reported in previous studies on single crystals (48% for FAP and 59% for S-FAP). For the 1.33  $\mu\text{m}$  wavelength, the Nd:S-FAP ceramics exhibited values approximately one order of magnitude lower than those of single crystals.

Because we did not explore the optimal conditions of the OC reflectivity for 1.33  $\mu\text{m}$  measurement, the efficiency could be improved by using optimal reflectivity, similar to the 1.06  $\mu\text{m}$  laser measurement. Additionally, while single crystals had AR coatings for both 1.06 and 1.33  $\mu\text{m}$ , ceramics of this study do not have this feature. Therefore, the application of AR coatings to reduce losses within the laser cavity is expected to improve laser properties. For instance, utilizing the  $\delta$  value estimated from the fitting curve in Figure 3, with Fresnel losses subtracted, to calculate laser output power using Eq. (2), could result in an expected increase in power of approximately three times.

In terms of maximum output, a direct comparison between the results of this study, which operated in the QCW mode (1% duty ratio), and those of single crystals operated in the CW

mode, is not easy. However, if this study were operated in the CW mode, and assuming there were no thermal issues, it was estimated that watt-level output exceeding those of single crystals could be achieved. To demonstrate this, we plan to implement an appropriate cooling system. Furthermore, we will evaluate the stability of output power during prolonged operation to enhance its practical applications.

In conclusion, laser behavior at a 1.06  $\mu\text{m}$  wavelength was studied with various output coupler reflectivities for non-cubic Nd:FAP and Nd:S-FAP ceramic materials. This study achieved the highest slope efficiencies to date: 10.1% for Nd:FAP and 11.7% for Nd:S-FAP ceramics. Laser operation at the 1.33  $\mu\text{m}$  wavelength was also achieved for both Nd:FAP and Nd:S-FAP, with slope efficiencies of 4.8% and 5.4%, respectively. Applying AR coatings, introducing a cooling system, and optimizing the cavity configuration—including evaluating the appropriate material thicknesses—will further improve laser performance.

### **Acknowledgments**

This work was partially supported by JST FOREST Program (JPMJFR203S) and JSPS KAKENHI (21H01611, 23K21035).

### **References**

- 1) R. C. Ohlmann, K. B. Steinbruegge, and R. Mazelsky, *Appl. Opt.* 7(5), 905 – 914 (1968).
- 2) K. B. Steinbruegge, T. Henningsen, R. H. Hopkins, R. Mazelsky, N. T. Melamed, E. P. Riedel, and G. W. Roland, *Appl. Opt.* 11(5), 999-1012 (1972).
- 3) X. X. Zhang, G. B. Loutts, M. Bass, and B. H. T. Chai, *Appl. Phys. Lett.* 64(1), 10-12 (1993).
- 4) X. X. Zhang, P. Hong, G.B. Loutts, J. Lefaucheur, M. Bass, and B.H.T. Chai, *Appl. Phys. Lett.* 64(24), 3205 – 3207 (1994).
- 5) S. Zhao, Q. Wang, X. Zhang, L. Sun, and S. Zhang, *Opt. Laser Technol.* 28(6), 477-480 (1996).
- 6) John B. Gruber, Clyde A. Morrison, Michael D. Seltzer, Andrew O. Wright, Melvin P. Nadler, Toomas H. Allik, J. Andrew Hutchinson, and Bruce H. T. Chai, *J. Appl. Phys.* 79(3), 1746-1758 (1996).
- 7) N. Faure, C. Borel, R. Templier, M. Couchaud, C. Calvat, and C. Wyon, *Opt. Mater.* 6(4), 293-303 (1996).
- 8) X. Zhang, S. Zhao, Q. Wang, L. Sun, S. Zhang, G. Yao, and Z. Zhang, *Opt. Commun.*

- 155(1-3), 55-60 (1998).
- 9) K.I. Schaffers, J.B. Tassano, A.B. Bayramian, and R.C. Morris, *J. Cryst. Growth* 253(1-4), 297-306 (2003).
  - 10) A. C. Erlandson, S. M. Aceves, A. J. Bayramian, A. L. Bullington, R. J. Beach, C. D. Boley, J. A. Caird, R. J. Deri, A. M. Dunne, D. L. Flowers, M. A. Henesian, K. R. Manes, E. I. Moses, S. I. Rana, K. I. Schaffers, M. L. Spaeth, C. J. Stolz, and S. J. Telford, *Opt. Mater. Exp.* 1(7), 1341-1352 (2011).
  - 11) M. Divoký, J. Pilař, M. Hanu, P. Navrátil, O. Denk, P. Severová, P. Mason, T. Butcher, S. Banerjee, M. D. Vido, C. Edwards, J. Collier, M. Smrž, and T. Mocek, *Opt. Lett.* 46(22), 5771-5773 (2021).
  - 12) T. Taira, *Opt. Mater. Exp.* 1(5), 1040-1050 (2011).
  - 13) R. Apetz, M. P. B. van Bruggen, *J. Am. Ceram. Soc.* 86(3), 480-486 (2003).
  - 14) J. Akiyama, Y. Sato, and T. Taira, *Opt. Lett.* 35(21), 3598-3600 (2010).
  - 15) J. Akiyama, Y. Sato, and T. Taira, *Appl. Phys. Exp.* 4(2), 022703 (2011).
  - 16) Y. Sato, M. Arzakantsyan, J. Akiyama, and T. Taira, *Opt. Mater. Exp.* 4(10), 2006-2015 (2014).
  - 17) Y. Sato, J. Akiyama, and T. Taira, *Sci. Rep.* 7(1), 10732 (2017).
  - 18) H. Furuse, N. Horiuchi, and B. N. Kim, *Sci. Rep.* 9(1), 10300 (2019).
  - 19) H. Furuse, T. Okabe, H. Shirato, D. Kato, N. Horiuchi, K. Morita, and B. N. Kim, *Opt. Mater. Exp.* 11(6), 1756-1762 (2021).
  - 20) H. Furuse, Y. Mochizuki, D. Kato, K. Morita, B. N. Kim, and T. S. Suzuki, *Scr. Mater.* 241, 115811 (2024).
  - 21) W. Koechner, *Solid State Laser Engineering*, Sixth Revised and Updated Edition, Springer Series in Optical Science (Springer, 2006).

## Figures

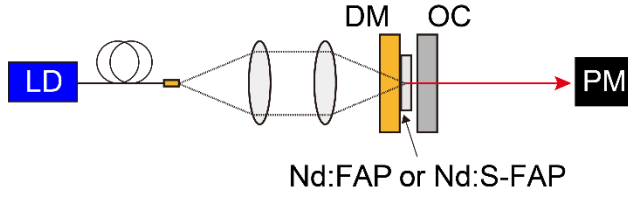


**Fig. 1.** Experimental setup for a laser cavity.

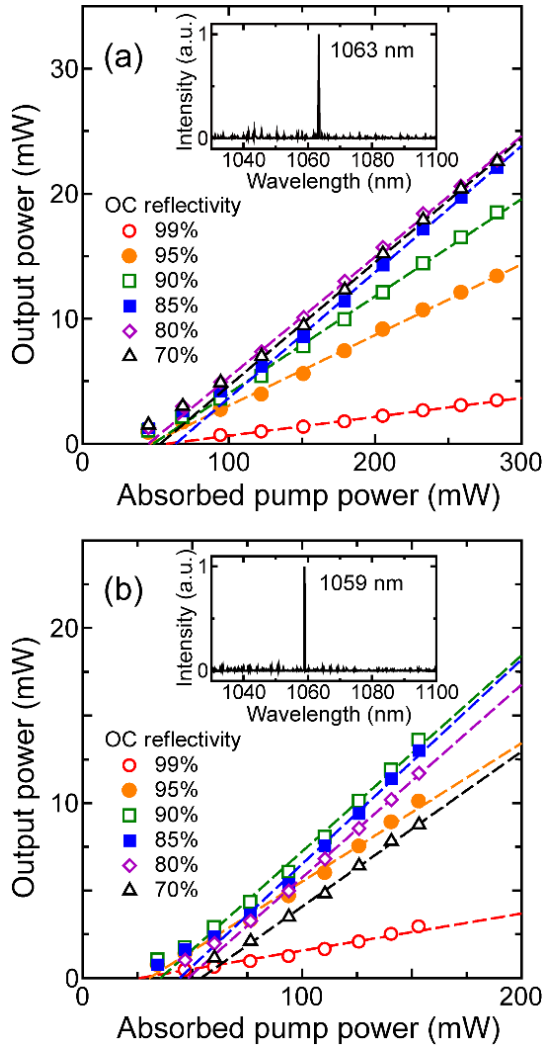


**Fig. 2.** Laser output power as a function of the absorbed pump power for (a) Nd:FAP ceramics and (b) Nd:S-FAP ceramics. Inset shows a typical lasing spectrum.



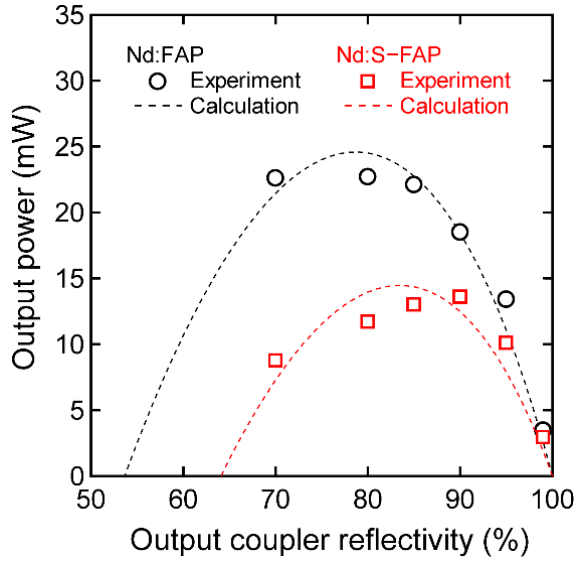


**Fig. 3.** Output power of laser relative to reflectance of OC.

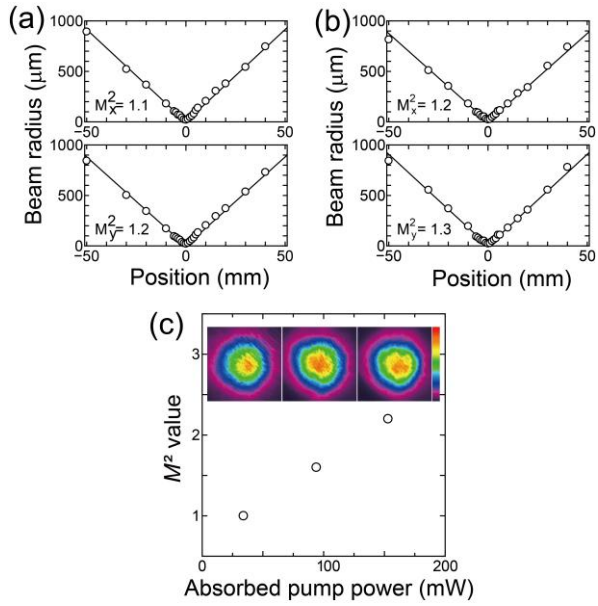


**Fig. 4.**  $M^2$  fitting curves for (a) Nd:FAP and (b) Nd:S-FAP beam profiles at absorbed pump powers of 94 and 47 mW, respectively. (c)  $M^2$  values for Nd:S-FAP ceramics with different absorbed pump powers.

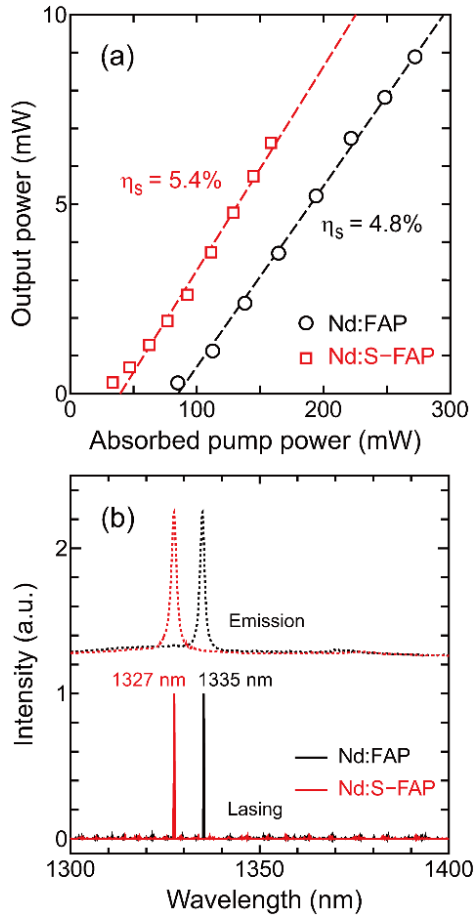


**Fig. 5.** Spectra and laser properties of Nd:FAP and Nd:S-FAP ceramics at 1.33  $\mu\text{m}$ . (a) Laser output power of Nd:FAP and Nd:S-FAP ceramics operating at 1.33  $\mu\text{m}$  as a function of the absorbed pump power. (b) Laser oscillation spectra of 1.33  $\mu\text{m}$  wavelength range by Nd:FAP and Nd:S-FAP.

**Table I.** Laser characteristics of the Nd:FAP and S-FAP single crystals and ceramics.

Host material	Laser wavelength (nm)	Slope eff. (%)	Output average power (mW)	Operation	Refs.
Nd:FAP ceramics	1063	10.1	22	QCW 1% Duty	This work
	1335	4.8	8.9		
Nd:S-FAP ceramics	1059	11.7	13	QCW 1% Duty	This work
	1327	5.4	6.6		
Nd:FAP single crystal	1063	48	$\approx 220$	CW	[3]
Nd:S-FAP single crystal	1059	59	$\approx 110$	CW	[4]
	1328	46	$\approx 85$		